Experimental and Numerical Analysis of the Cyclic Behaviour of RC Beam-Column Connections with Plain Reinforcing Bars

C. Fernandes, J. Melo, H. Varum & A. Costa
University of Aveiro, Portugal

SUMMARY:
The information available in the literature about the cyclic behaviour of reinforced concrete elements with plain reinforcing bars is scarce. As a consequence, the influence of bar slippage in elements with plain bars is not yet comprehensively understood. In this paper are presented and discussed the main results of the cyclic tests carried out on five full-scale reinforced concrete beam-column joints with plain bars and without specific detailing for seismic demands. An additional joint specimen with deformed bars was also tested for comparison. Furthermore, numerical models were built to simulate the response of two of the specimens. Particular attention was given to the influence of bar slippage. The results of the conducted analyses underline the importance of accounting for bond-slip in the numerical modelling of elements with plain bars and also highlight the need for specific models to simulate the effects of this mechanism in the presence of plain bars.

Keywords: Beam-column joints, Plain reinforcing bars, Cyclic testing, Numerical modelling, Bond-slip

1. INTRODUCTION

The hysteretic behaviour of reinforced concrete (RC) structures is strongly dependent on the interaction between the concrete and the steel reinforcement. Cyclic load reversals, like those induced by earthquakes, lead to progressive bond degradation and consequent relative slippage between the reinforcing bars and the surrounding concrete (bond-slip). RC elements with plain reinforcing bars, present in a significant number of existing RC building structures designed and built before the 1970s all over the world (hence prior to the enforcement of the modern seismic-oriented design philosophies) are particularly sensitive to the effects of bar slippage. However, when compared to the amount of information provided in the literature for elements with deformed bars, the data available for elements with plain bars (Fernandes *et al.*, 2011; Melo *et al.*, 2011; Bedirhanoglu *et al.*, 2010; Verderame *et al.*, 2008; Varum, 2003; Pampanin *et al.*, 2001) is scarce. Moreover, perfect bond between concrete and steel is commonly assumed in the analysis of RC structures, which may lead, for example, to lateral deformations significantly smaller than the real element deformations or to lateral stiffness larger than the existing element stiffness (Sezen and Setzler, 2008). Several modelling strategies that allow taking into account the effects of bar slippage are proposed in the literature (like in Lowes and Altoontash, 2003, and Youssef and Ghobarah, 2001), but the majority was developed based on data concerning elements with deformed bars. Due to the differences in the interaction mechanisms at the concrete-steel interface between elements with deformed bars and elements with plain bars, such models may not be adequate for the latter. As a consequence of the lack of experimental data and of general and reliable models for simulating bond-slip effects, the influence of the bond properties of plain bars on the hysteretic behaviour of existing RC structures is not yet comprehensively understood.

In this framework, in this paper are presented and discussed the main results of the cyclic tests carried out on five full-scale RC interior beam-column connections built with plain reinforcing bars and without specific detailing for seismic demands. An additional joint specimen built with deformed bars was also tested for establishing the performance comparison with the analogous specimen with plain

bars. The parameters under investigation were the bond properties (plain bars versus deformed bars), displacement history, column axial load, and amount of steel reinforcement in the elements. In addition to the experimental campaign, nonlinear fibre-based numerical models, calibrated with the tests results, were built to simulate the cyclic response of the two analogous joint specimens, one with plain bars and the other with deformed bars. A simple modelling strategy presented in the literature, the development and calibration of which was based on data referring to elements with deformed bars, was adopted to include the effects of bar slippage in the analysis of the joint specimen with plain bars. The comparisons established between the numerical and experimental results allowed to investigate about the importance of accounting for bond-slip and also check the adequacy of the adopted model. Detailed information about the experimental and numerical work described in this paper, including additional analysis of the experimental results, can be found in (Fernandes, 2012).

2. TESTING CAMPAIGN

2.1. Test specimens

The joint specimens were designed to represent interior beam-column connections in existing RC building frame structures designed and built before the 1970s, without specific detailing for seismic demands. In each specimen: each beam element represents a half-span beam, with length equal to 2 m and 0.30x0.40 m^2 cross-section; and, each column element represents a half-storey column, with length equal to 1.5 m and 0.30x0.30 m^2 cross-section. The specimens were built full-scale. Five specimens were built with plain reinforcing bars (JPA-1, JPA-2, JPA-3, JPB and JPC). One additional specimen (JD) was built with deformed bars. All the other characteristics of JD were made equal to those of JPA-1. Fig. 2.1 depicts the dimensions and reinforcement detailing of the joint specimens. Specimens JPA-1, JPA-2, JPA-3, and JD were built with the same amount of steel reinforcement, which is referred to herein as standard amount. In comparison with the previous specimens, JPB and JPC were built with twice the amount of column longitudinal reinforcement. JPC was also built with twice the amount of transverse reinforcement in the beams and 2.5 times the transverse reinforcement in the columns. In all specimens the stirrups were bent with 90º bends, the longitudinal reinforcement of the elements was continuous ending with 90º bends, and there was no transverse reinforcement in the joint region. The concrete cover over transverse reinforcement was equal to 20 mm in the beams and columns.

The six joint specimens were cast on the same day, with the same concrete mixture. Compressive tests on cubic concrete samples, cast together with the specimens, were conducted to determine the concrete compressive strength. The mean value obtained for the concrete strength is equal to 23.8 MPa with a coefficient of variation equal to 4%. Regarding the mechanical properties of the steel reinforcement, Table 2.1 shows the mean values obtained for the longitudinal bars resorting to tensile strength tests.

Table 2.1. Mechanical properties of the steel reinforcement (mean values)

Characteristics	Plain bars	Deformed bars
Yielding strength (MPa)	590	480
Ultimate strength (MPa)	640	601
Elastic modulus (GPa)	198	199

2.2. Test setup and loading pattern

The joint specimens were tested horizontally (Fig. 2.2). Four high load-carrying capacity devices with reduced friction were placed below the specimens to carry their self-weight. Steel reaction frames associated to sliding devices at the beams extremities and to a pinned connection at the base of the column were used to simulate the support conditions. Two hydraulic actuators were arranged at the column top, one to impose the lateral loading and the other for the axial load. Linear Variable Displacement Transducers (LVDTs) were used to monitor the lateral displacements of the beams and columns, and the local deformation and evolution of crack opening at the joint region and vicinities.

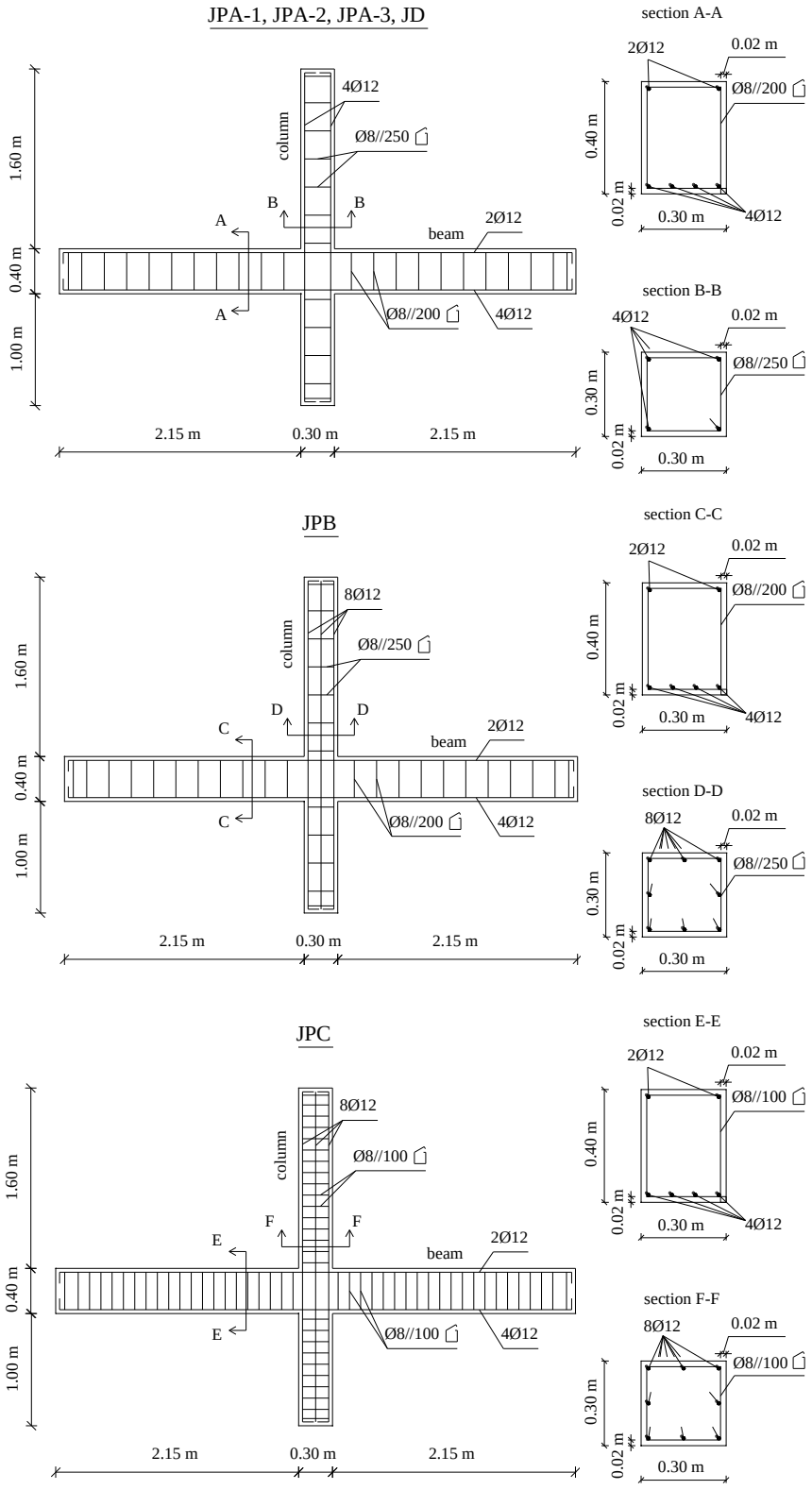

Figure 2.1. Dimensions and reinforcement detailing of the beam-column joint specimens

The quasi-static cyclic tests were carried out under displacement-controlled conditions. The joint specimens were subjected to a lateral displacement history (d_c) imposed on the free end of the superior column, and to constant axial load (N) applied on the top of the column. Two displacement histories (see Fig. 2.2), both up to 120 mm (4% drift) but with different number of displacement levels, were considered in order to assess the influence of magnitude of drift interval and of number of cycles on

the specimens' response, namely on the degradation of stiffness and strength. Specimen JPA-2 was tested under displacement history type 2. The other joint specimens were tested under displacement history type 1. Two levels of axial load were also considered: 200 kN (normalized axial load equal to 9.4%), in JPA-1, JPA-2 and JD, representative of 2-3 storey buildings; and, 450 kN (normalized axial load equal to 21.3%), in JPA-3, JPB and JPC, representative of 4-5 storey buildings.

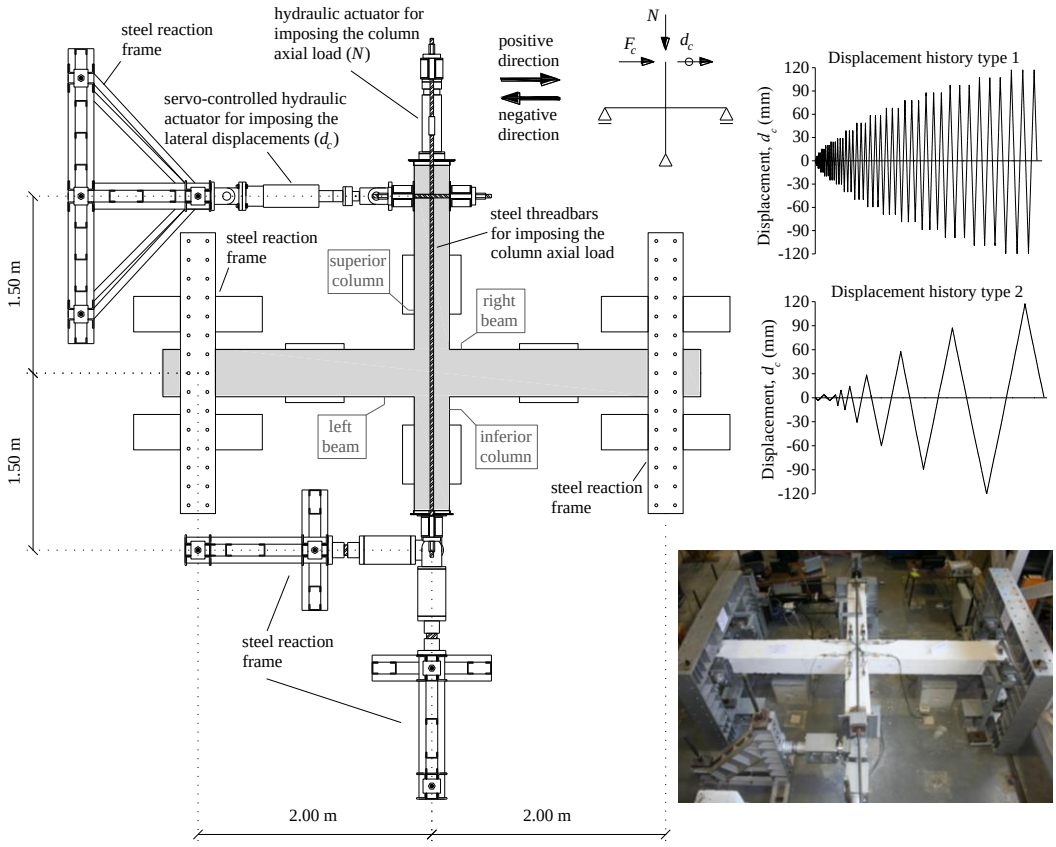

Figure 2.2. Test setup

3. ANALYSIS OF EXPERIMENTAL RESULTS

Fig. 3.1 depicts the experimental results in terms of lateral load versus imposed drift. Table 3.1 indicates for each specimen: the maximum lateral load ($F_{c,max}$); the drift level ($\Delta_{Fc,max}$) at which $F_{c,max}$ was registered; and, the maximum strength degradation ($\Delta F_{4\%}$), computed as the ratio between the lateral load at maximum drift and $F_{c,max}$. It should be noted that the specimens' response was not perfectly symmetrical and that results in Table 3.1 refer to the positive loading direction.

Table 3.1. Maximum lateral load and maximum strength degradation registered for the joint specimens

Specimen	$F_{c,max}$ (%)	$\Delta F_{c,max}$ (%)	$\Delta F_{4\%}$ (%)
JPA-1	34.0	3.3	4.5
JPA-2	35.8	3.0	5.8
JPA-3	43.3	2.7	26.6
JPB	39.5	2.3	15.8
JPC	38.3	3.3	10.0
JD	39.0	2.0	19.0

Specimen JPA-3 displayed the largest lateral strength and also the greatest strength degradation after the maximum lateral load. Within the drift range under analysis, only for this specimen was registered the conventional failure condition corresponding to 20% reduction in strength. Small differences in stiffness were registered between the joint specimens with plain bars. The pinching effect was evident

for all specimens, being less important for the specimen with deformed bars and particularly evident in the response of specimens JPB and JPC.

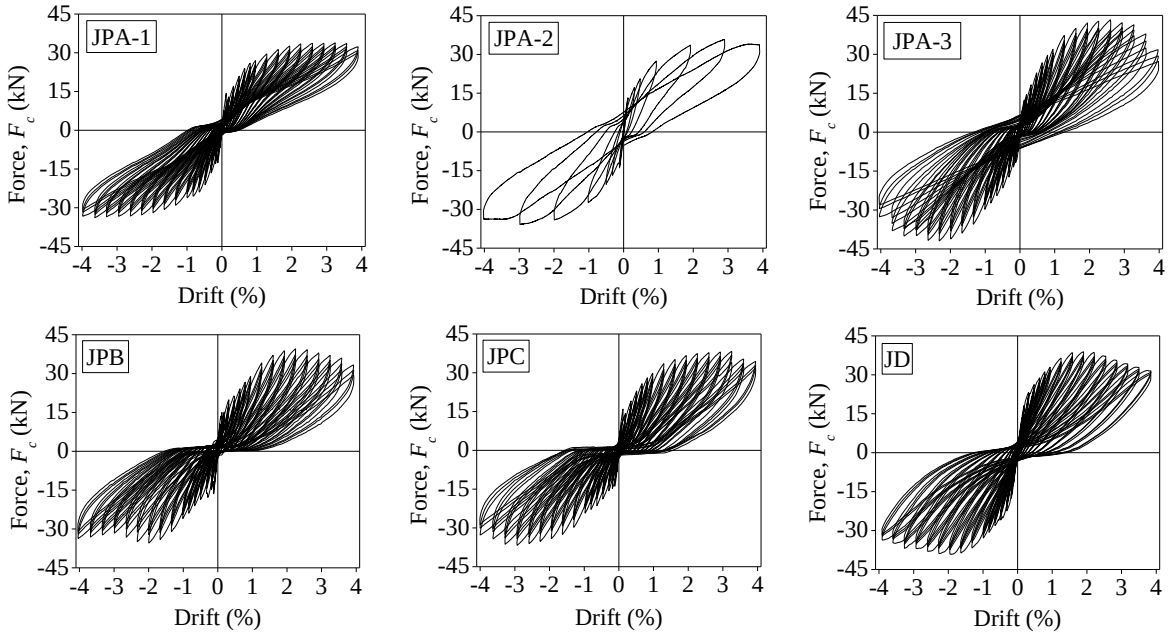

Figure 3.1. Lateral load versus drift diagrams

Fig. 3.2 illustrates the crack pattern corresponding to the final damage state in the specimens. In general terms, the specimens with plain reinforcing bars displayed damage concentrated at the beam-joint and column-joint interfaces. In specimen JPA-3, severe cracking in the joint region, with concrete cover spalling, was also observed; despite a few inclined cracks with relatively small opening, the damage in the joint region was mainly defined by two diagonal cracks. In specimens JPB and JPB, damage was mainly concentrated at the beam-joint interfaces and damage in the columns was minor. Conversely, the specimen with deformed bars displayed a more widely spread damage distribution. In this specimen, cracking was spread along the length of the elements and several inclined cracks with relatively small opening were developed in the joint region.

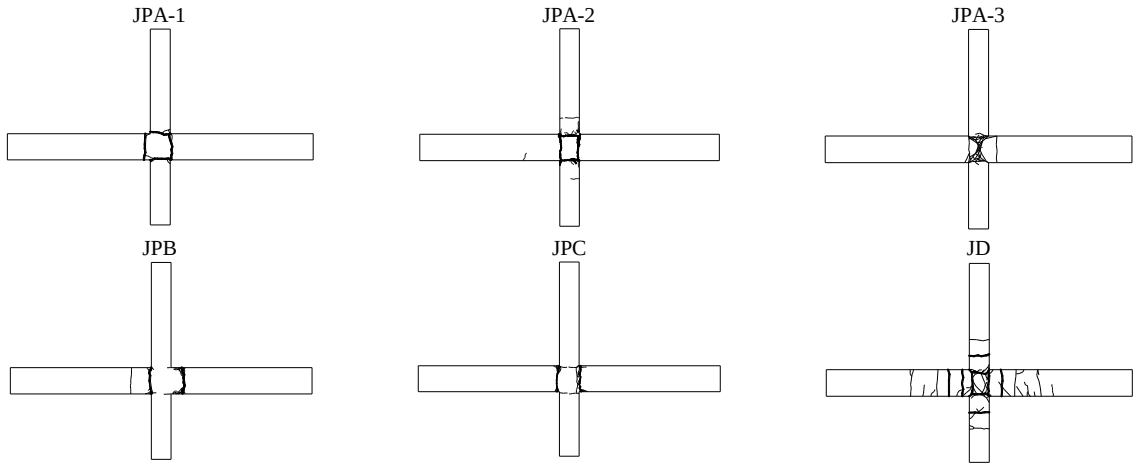

Figure 3.2. Crack pattern corresponding to the final damage state

The evolution of dissipated energy, computed as the area under the lateral load-drift diagrams, is plotted in Fig. 3.3 for all specimens except JPA-2 (excluded from this analysis since it was tested under a displacement history different from that imposed on the other specimens). Fig. 3.3 shows that the evolutions of dissipated energy are similar up to 2% drift. Afterwards, the energy dissipation

associated with JPA-3 increases with relatively higher rate. At the maximum imposed drift, the energy dissipated by JPA-3 is about 1.5 times the energy dissipated by each of the other joint specimens with plain bars, and 1.4 times the energy dissipated by the joint specimen with deformed bars.

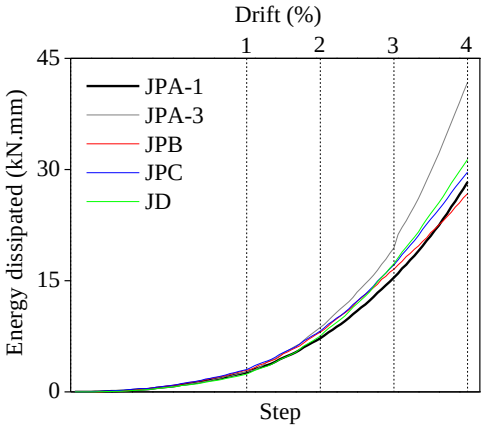

Figure 3.3. Evolution of dissipated energy

In order to conclude about the sensitivity of the specimens' response to the varying parameters, comparison was established between the results of specimens: JPA-1 and JPA-2 (displacement history); JPA-1 and JPA-3 (axial load); JPA-1 and JD (bond properties); JPA-3 and JPB, and JPB and JPC (amount of steel reinforcement). The main conclusions are presented in the next paragraphs.

The influence of displacement history was minor. Specimens JPA-1 and JPA-2 displayed similar values of maximum lateral load and lateral load at the maximum imposed drift, and similar secant stiffness (measured for the peak load in the cycles with the same drift level) and damage distribution.

The increase in column axial load in JPA-3 led to: increase of 27% in the maximum lateral load; more pronounced strength degradation after the maximum lateral load mainly due to the severe damage developed in the joint region; increase in stiffness; reduction in the pinching effect; and, significant increase in energy dissipation (of 50% at the maximum imposed drift).

The influence of bond properties was particularly shown by the differences in damage distribution. An improvement of the bond properties (JD) led to: increase of 15% in the maximum lateral load; more pronounced strength degradation after the maximum lateral load; increase in stiffness; reduction in the pinching effect; and, increase in the energy dissipation (of about 10% at the maximum imposed drift).

The influence of the amount of steel reinforcement was particularly shown by the differences in damage distribution. Increasing the amount of column longitudinal reinforcement had a more significant influence than increasing the amount of transverse reinforcement in the elements. In this case (JPB): the maximum lateral load was reduced in 9%; the strength degradation after the maximum lateral load was less pronounced; the stiffness was reduced; the pinching effect was considerably more evident; and, the energy dissipation was significantly reduced (in about 50% at the maximum imposed drift).

4. NUMERICAL MODELLING

This section addresses the numerical modelling of the cyclic behaviour of the two analogous joint specimens, JPA-1 and JD. Nonlinear fibre-based models were built using the SeismoStruct (SeismoSoft, 2012) software and calibrated with the experimental results. Firstly, a model was calibrated for specimen JD without taking into account the bond-slip mechanism. Then, the calibrated model was adopted to simulate the response of specimen JPA-1 and only the yield strength of the steel

reinforcement was changed. Secondly, a simple modelling strategy proposed in the literature to simulate the effects of bar slippage, the development and calibration of which was based on data referring to elements with deformed bars, was implemented in the model previously adopted for specimen JPA-1. The main objectives of the analyses were to confirm the importance of considering bond-slip towards a more accurate simulation of the cyclic behaviour of the joint specimen with plain bars, and check the adequacy of the strategy adopted to incorporate the effects of bar slippage in the presence of this type of steel reinforcement.

4.1. Numerical model without bond-slip effects

In the model, each structural element was represented by five displacement-based elements with distributed plasticity, the cross-sections of which were divided into 250 longitudinal fibres. The cross-sectional dimensions, steel reinforcement detailing, and support conditions adopted are representative of those described in Section 3. The joint region was modelled as rigid. This assumption can be considered adequate for JPA-1 since damage in the joint region of this specimen was not observed, but not appropriate for JD (for which joint shear deformation should not be disregarded). However, for comparison with JPA-1 and considering that the numerical analysis herein presented intended to focus on the effects of bar slippage, the rigid joint assumption was also adopted for JD.

The model adopted for the concrete follows the constitutive relationship proposed by Mander *et al.* (1988) with the cyclic rules proposed by Martinez-Rueda and Elnashai (1997). Table 4.1 gives the values adopted for the model parameters, namely: cylinder compressive strength (f_c); tensile strength (f_t); strain at peak stress (ε_c); confinement factor (k_c); and, specific weight (γ).

Table 4.1. Values adopted for the concrete model parameters

Concrete	f_c (MPa)	f_t (MPa)	ε_c (mm/mm)	k_c	γ (kN/m^3)
Unconfined	19	2.9	0.0022	1	24
Confined				1.04	

The model adopted for the steel reinforcement is based on the Menegotto-Pinto model (1973) coupled with the isotropic hardening rules proposed by Filippou *et al.* (1983). Table 4.2 gives the values adopted (and values recommended in SeismoStruct) for the model parameters, namely: modulus of elasticity (E_s); yield strength (f_y); strain hardening parameter (μ); transition curve initial shape parameter (*R0*); transition curve shape calibrating coefficients (*a1* and *a2*); isotropic hardening calibrating coefficients (*a3* and *a4*); fracture/buckling strain (ε_{ult}); and, specific weight (γ).

Table 4.2. Values adopted for the steel model parameters

Model parameter	Recommended value/range	Adopted value	
		Deformed bars (JD)	Plain bars (JPA-1)
E_s (GPa)	-	200	
f_y (MPa)	-	455	590
(μ)	0.005 - 0.015	0.008	
R0	-	19.5	
a1	18.5	18.8	
a2	0.05 - 0.15	0.15	
a3	0.01 - 0.025	0	
a4	2 - 7	1	
ε_{ult}	-	0.1	
γ (kN/m^3)	-	78	

The loading conditions in the numerical model simulate those imposed in the cyclic tests, that is: constant column axial load equal to 197 MPa (mean value registered in the cyclic tests); and, lateral displacement history type 1 (shown in Fig. 2.2) imposed on the end node of the superior column.

Fig. 4.1 and Fig. 4.2 depict, for JD and JPA-1 respectively, the comparison between the numerical and experimental results in terms of lateral load-drift diagrams and moment-curvature (mean values)

diagrams computed for the beam/column interface sections. The main conclusion drawn from the comparative analyses were: i) for both specimens, the models show important shortcomings; namely, strength degradation is not represented, and the stiffness of the reloading branches, the pinching effect and the moment-curvature relationship of the beams are poorly reproduced; ii) in general terms, the peak envelope of specimen JD is properly reproduced, namely in terms of maximum lateral load and tangent stiffness; iii) the differences between the numerical and experimental results are considerably increased when the model calibrated for JD with the yield strength of the plain bars is adopted to simulate the response of JPA-1, namely in terms of maximum lateral load, stiffness, pinching effect, and moment-curvature relationships; iv) the cracking distribution in the numerical models occurs along almost the entire length of the beams and columns, therefore contrarily to what was experimentally observed for JPA-1.

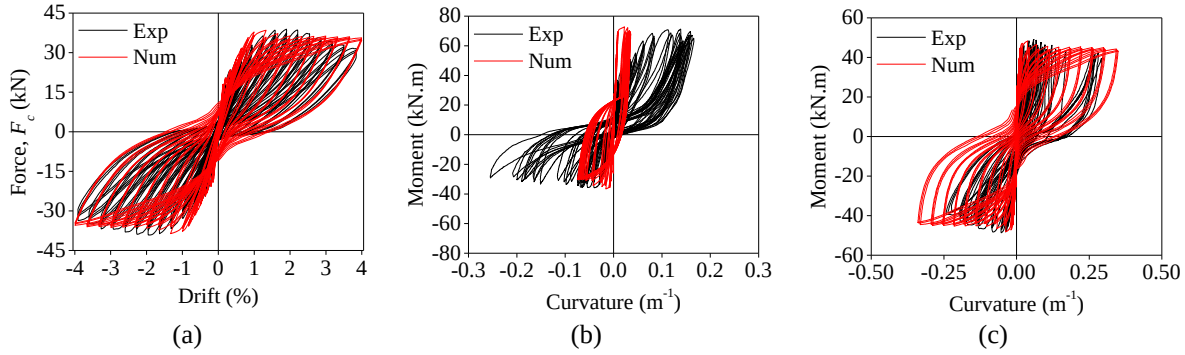

Figure 4.1. Comparison between numerical and experimental results of specimen JD: a) lateral load-drift diagram; b) moment-curvature (mean values) diagram for the beam-joint interface sections; c) moment-curvature (mean value) diagram for the column-joint interface sections

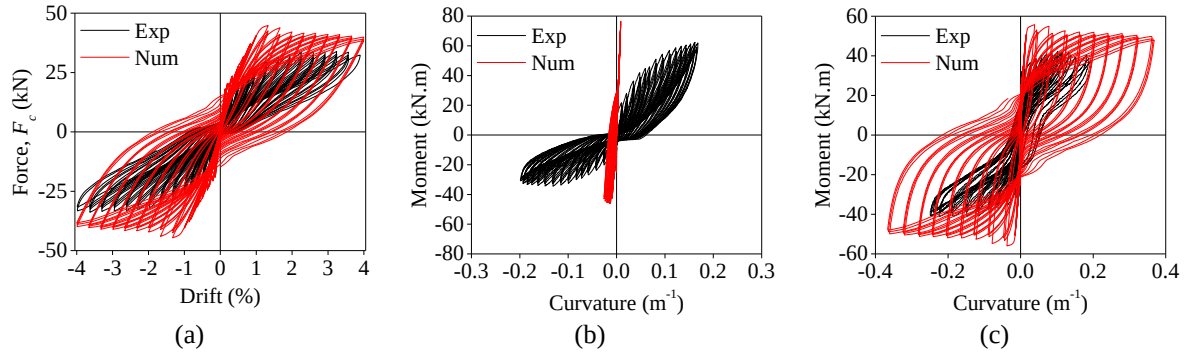

Figure 4.2. Comparison between numerical and experimental results of specimen JPA-1: a) lateral load-drift diagram; b) moment-curvature (mean values) diagram for the beam-joint interface sections; c) moment-curvature diagram (mean values) for the column-joint interface sections

4.2 Numerical model with bond-slip effects

Based on the modelling strategy proposed by Yu (2006), which in turn was developed based on the joint model proposed by Lowes and Altoontash (2003), rotational springs (fitted in the beam-joint and column-joint interfaces) were implemented in the model of specimen JPA-1 to account for the effects of the bond-slip mechanism (Fig. 4.3). A moment-rotation relationship was assigned to each spring.

The joint model proposed by Lowes and Altoontash (2003) includes a general one-dimensional constitutive model (force-displacement response envelope, unload-reload paths and damage rules) for the springs, which is not available in SeismoStruct. Therefore, among the several models included in SeismoStruct: an asymmetric bilinear model was adopted for the springs in the beams, however not featuring degradation of either strength or stiffness; and, for the springs in the columns, a model consisting on a bilinear simplification of the model proposed by Takeda *et al.* (1970), with parameters

to control degradation of stiffness but not degradation of strength. The corresponding moment-rotation relationships were first derived based on the bar stress-slip and bar stress-spring force relationships proposed by Lowes and Altoontash (2003), which were established based on data concerning elements with deformed bars and assuming the longitudinal reinforcement anchored in the joint region. This methodology applied to JPA-1 led to a poor simulation of the specimen's response, with the corresponding numerical results being similar to those obtained from the model without the springs. This is considered to be mainly due to the differences in the concrete-steel interaction mechanisms between elements with plain and deformed bars. The parameters of the spring models were then calibrated to fit the experimental results, namely the lateral load-drift and moment-curvature diagrams. Fig. 4.4 depicts the comparison between the numerical and experimental results.

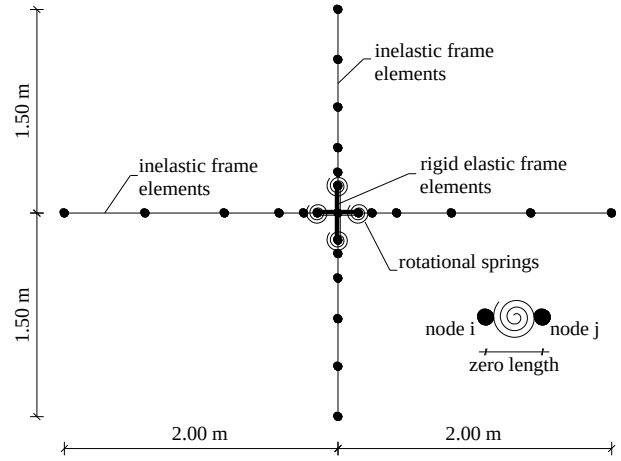

Figure 4.3. Model with rotational springs adopted for specimen JPA-1

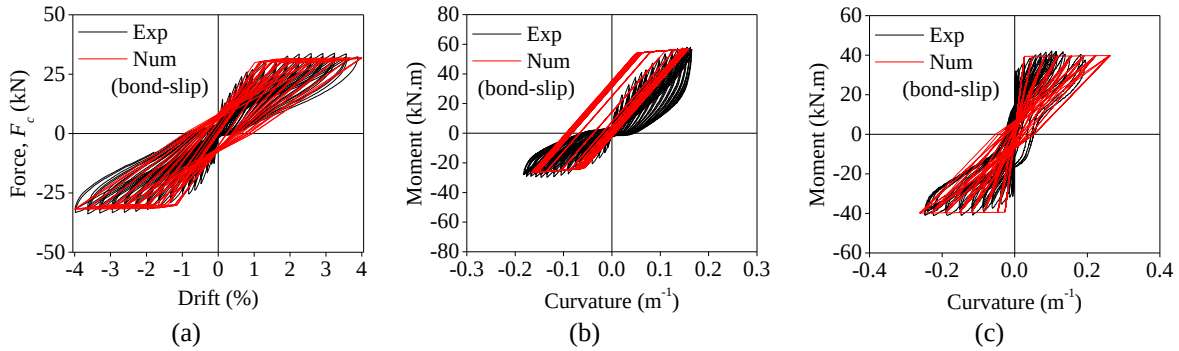

Figure 4.4. Comparison between numerical (considering bond-slip) and experimental results of specimen JPA-1: a) lateral load-drift diagram; b) moment-curvature (mean values) diagram for the beam-joint interface sections; c) moment-curvature (mean values) diagram for the column-joint interface sections

The analysis of Fig. 4.2 and Fig. 4.4 shows that, by considering the bond-slip effects: i) a better simulation of the lateral load-drift enveloped is obtained, as well as of the stiffness of the loading and unloading branches; ii) the difference in maximum load between the numerical and experimental results is reduced from 32% to 6%; iii) the differences in maximum moment are reduced from 23% to 2% for the beams, and from 32% to 6% for the columns; iv) the differences in maximum curvature of the beams are reduced from 95% to 2% in the positive moment direction, and from 87% to 10% in the negative moment direction; v) the differences in maximum curvature of the columns are reduced from 90% to 37% in one moment direction, and from 47% to 6% in the other moment direction. However, despite the general better approximation to the experimental results attained by including bond-slip in the model, the numerical results show the inadequacy of the models adopted for the rotational springs. More adequate models should be hence implemented in SeismoStruct, featuring a more refined envelope curve, as well as appropriate parameters to control the stiffness and strength degradations.

5. FINAL COMMENTS

The experimental results obtained in the framework of the investigation work described in this paper contribute to the existing database on the cyclic behaviour of RC elements with plain reinforcing bars. The results of the numerical analyses underline the importance of taking into account the influence of bond-slip in the numerical modelling of RC elements with plain bars. Moreover, they highlight the inadequacy of current modelling strategies developed for elements with deformed bars to incorporate the effects of bar slippage in the analysis of elements with plain bars, and therefore the need for specific models to account for bond-slip in the presence of this type of steel reinforcement.

AKCNOWLEDGEMENT

This paper reports research developed under financial support provided by "FCT - Fundação para a Ciência e Tecnologia", Portugal, co-funded by the European Social Fund within the scope of the POPH program of the National Strategic Reference Framework, namely through the PhD grant of the first author, with reference SFRH/BD/27406/2006. The authors also acknowledge the research project SPARCS, with reference PTDC/ECM/101201/2008. In addition, the authors acknowledge: Eng. António Figueiredo, Eng. Henrique Pereira, Eng. Hugo Rodrigues, and Eng. Randolph Borg for their assistance in the experimental programme and numerical modelling; and, the companies Civilria, Grupo Meneses, Paviútil, Silva Tavares & Bastos Almeida, and Somague for the construction of the test specimens and structural reaction elements.

REFERENCES

Bedirhanoglu, I., Ilki, A., Pujol, S. and Kumbasar, N. (2010). Behavior of Deficient Joints with Plain Bars and Low-Strength Concrete. *ACI Structural Journal*. **107:3**, 300-10.

Fernandes, C. (2012). Cyclic behaviour of RC elements with plain reinforcing bars. PhD Thesis, University of Aveiro, Portugal.

Fernandes, C., Melo, J., Varum, H. and Costa, A. (2011). Comparative analysis of the cyclic behavior of beam-column joints with plain and deformed reinforcing bars. *IBRACON Structures and Materials Journal*. **4:1**, 147-172.

Lowes, L. and Altoontash, A. (2003). Modeling Reinforced-Concrete Beam-Column Joints Subjected to Cyclic Loading. *Journal of Structural Engineering*. **129**:12, 1686-1697.

Mander, J.B., Priestley, M.J.N. and Park, R. (1988). Theoretical Stress-Strain Model for Confined Concrete. *Journal of Structural Engineering*. **114:8**, 1804-1826.

Martínez-Rueda, J.E. and Elnashai, A.S. (1997). Confined Concrete Model under Cyclic Loads. *Materials and Structures*. **30:3**, 139-147.

Melo, J., Fernandes, C., Varum, H., Rodrigues, H., Costa, A., and Arêde, A. (2011). Numerical modelling of the cyclic behaviour of RC elements built with plain reinforcing bars. *Engineering Structures*. **33:2**, 273-286.

Menegotto, M. and Pinto, P. (1973). Method of Analysis for Cyclically Loaded Reinforced Concrete Plane Frames Including Changes in Geometry and Non-Elastic Behaviour of Elements under Combined Normal Force and Bending. *IABSE Symposium: Resistance and Ultimate Deformability of Structures Acted on by Well Defined Repeated Loads*.

Pampanin, S., Calvi, G.M. and Moratti, M. (2001). Seismic Behavior of RC Beam-Column Joints Designed for Gravity Loads. *12th European Conference on Earthquake Engineering*. Paper No. 726.

SeismoSoft (2012). Seismostruct - A Computer Programme for Static and Dynamic Nonlinear Analysis of Framed Structures. *Available from URL: http://www.seismosoft.com*.

Sezen, H. and Setzler, E.J. (2008). Reinforcement slip in reinforced concrete columns. *ACI Structural Journal*. **105:3**, 280-289.

Takeda, T., Sozen, M.A. and Nielsen, N.N. (1970). Reinforced Concrete Response to Simulated Earthquakes. *Journal of Structural Division, ASCE*. **96**:**ST12**, 2557-2573.

Varum, H. (2003). Seismic assessment, strengthening and repair of existing buildings. PhD Thesis, University of Aveiro, Portugal.

Verderame, G.M., Fabbrocino, G. and Manfredi, G. (2008). Seismic response of R.C. columns with smooth reinforcement. Part II: Cyclic tests. *Engineering Structures*. **30:9**, 2008, 2289-300.

Youssef, M. and Ghobarah, A. (2001). Modelling of RC Beam-Column Joints and Structural Walls. *Journal of Earthquake Engineering*. **5:1**, 93-111.

Yu, W. (2006). Inelastic Modeling of Reinforcing Bars and Blind Analysis of the Benchmarks Tests on Beam-Column Joints under Cyclic Loading. Master's Dissertation, Rose School, Pavia.